Synthesis and Structural Characterisation of Some *Triangulo*- and Binuclear Clusters of Platinum from the Reaction of $[Pt_3(\mu\text{-}SO_2)_3\{P(C_6H_{11})_3\}_3]$ with 2,6-Xylyl Isocyanide†

D. Michael P. Mingos,* Ian D. Williams, and Michael J. Watson
Inorganic Chemistry Laboratory, University of Oxford, South Parks Road, Oxford OX1 3QR

The compound $[Pt_3(\mu\text{-}SO_2)_3\{P(C_6H_{11})_3\}_3]$ reacts with 2 mol of 2,6-xylyl isocyanide, CNC_8H_9, to give $[Pt_3(\mu\text{-}SO_2)_2(CNC_8H_9)_2\{P(C_6H_{11})_3\}_3]$ (**1**) and with an excess of isocyanide to give $[Pt_2(\mu\text{-}SO_2)(CNC_8H_9)_2\{P(C_6H_{11})_3\}_2]$ (**2**). The molecular structures of both compounds have been determined by single-crystal *X*-ray techniques using diffractometer data. Compound (**1**) crystallises in the monoclinic space group $P2_1$ with two units of formula $[Pt_3(SO_2)_2(CNC_8H_9)_2\{P(C_6H_{11})_3\}_3]\cdot 3MeCN\cdot CH_2Cl_2$ in a cell of dimensions a = 14.957(5), b = 24.604(4), c = 13.035(2) Å, and β = 114.28(2)° and (**2**) in the monoclinic space group $P2_1/n$ with four units of formula $[Pt_2(SO_2)(CNC_8H_9)_2\{P(C_6H_{11})_3\}_2]\cdot 1.5CH_2Cl_2$ in a cell of dimensions a = 14.842(1), b = 25.394(3), c = 17.270(2) Å, and β = 112.16(1)°. The structure of (**1**) is based on an isosceles triangle of platinum atoms, with the two shorter Pt–Pt edges [av. 2.727(1) Å] bridged by SO_2 ligands and the longer edge [2.8422(9) Å] unbridged. The isocyanide ligands are co-ordinated to the platinum atoms which define this long bond. N.m.r. studies ($^{31}P\text{-}\{^1H\}$ and $^{195}Pt\text{-}\{^1H\}$) have confirmed that this structure is retained in solution. In (**2**) the platinum–platinum bond has a length of 2.6934(5) Å and is bridged by a SO_2 ligand. The co-ordination environments about each platinum atom are completed by a $P(C_6H_{11})_3$ ligand and a terminal CNC_8H_9 ligand. N.m.r. data ($^{31}P\text{-}\{^1H\}$ and $^{195}Pt\text{-}\{^1H\}$) for this compound in solution have been recorded. The formation of (**1**) and (**2**) from $[Pt_3(SO_2)_3\{P(C_6H_{11})_3\}_3]$ is quite unexpected in view of earlier studies on $[Pt_3(\mu\text{-}CO)_3\{P(C_6H_{11})_3\}_3]$ with the same isocyanide ligand. The 44-valence-electron structure observed for (**1**) has no precedent in platinum cluster chemistry and the isolation of the dimeric compound (**2**) underlines the importance of degradation processes in ligand-substitution reactions.

Although a large number of 42- and 44-electron *triangulo*-platinum cluster compounds have been characterised,[1,2] their substitution chemistry has not been extensively studied. The investigations of the substitution reactions of $[Pt_3(CO)_3(PBu^t_3)_3]$, $[Pt_3(CO)_3\{P(C_6H_{11})_3\}_3]$, $[Pt_3(SO_2)_3(PPh_3)_3]$, and $[Pt_3(CO)_3(PPh_3)_4]$ with SO_2, CS_2, CNR, and other phosphine ligands[1,3–5] have demonstrated that these reactions are by no means straightforward. In particular, fragmentation reactions proceed at approximately the same rate as substitution reactions. Farrar and co-workers[3] noted that $[Pt_3(CO)_3(PBu^t_3)_3]$ fragments immediately when treated with small molecules such as CS_2, OCS, and SO_2, even under mild conditions (−25 °C). In contrast, the study of the reaction of $[Pt_3(CO)_3(PPh_3)_4]$ with SO_2 at 60 °C provided no evidence of fragmentation and $[Pt_3(SO_2)_3(PPh_3)_3]$ was isolated as the sole product.[4] Similarly, $[Pt_3(CO)_3\{P(C_6H_{11})_3\}_3]$ reacts with 3 and 5 mol of 2,6-xylyl isocyanide to give $[Pt_3(\mu\text{-}CO)(\mu\text{-}CNC_8H_9)_2(CNC_8H_9)\{P(C_6H_{11})_3\}_2]$ and $[Pt_3(\mu\text{-}CNC_8H_9)_3(CNC_8H_9)_2\{P(C_6H_{11})_3\}]$ respectively.[1] In these compounds the bridging isocyanide ligands are severely bent about the nitrogen atoms and their steric requirements are incompatible with the presence of $P(C_6H_{11})_3$ ligands on both of the metal atoms being bridged. Therefore, it has been argued that replacement of a bridging CO by isocyanide labilises an adjacent terminal $P(C_6H_{11})_3$ ligand. In order to gain a greater understanding of these substitution reactions we have investigated the reactions of $[Pt_3(SO_2)_3\{P(C_6H_{11})_3\}_3]$ with CNC_8H_9.

Results and Discussion

The reactions of $[Pt_3(\mu\text{-}SO_2)_3\{P(C_6H_{11})_3\}_3]$ with 2,6-xylyl isocyanide are summarised in Scheme 1. Two major products, whose relative yields depend on the mole ratios of the reactants, are isolated from the reactions. Compound (**1**) is a 44-electron

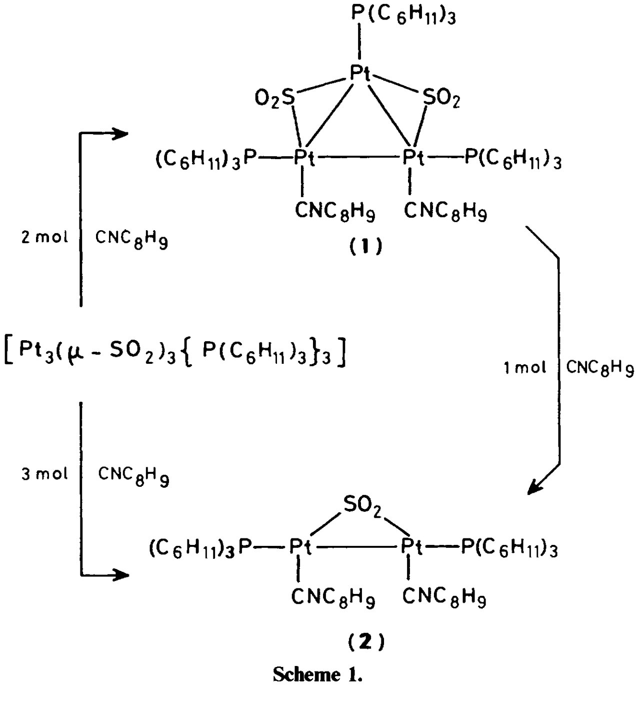

Scheme 1.

---

† *Supplementary data available:* see Instructions for Authors, *J. Chem. Soc., Dalton Trans.*, 1988, Issue 1, pp. xvii—xx.

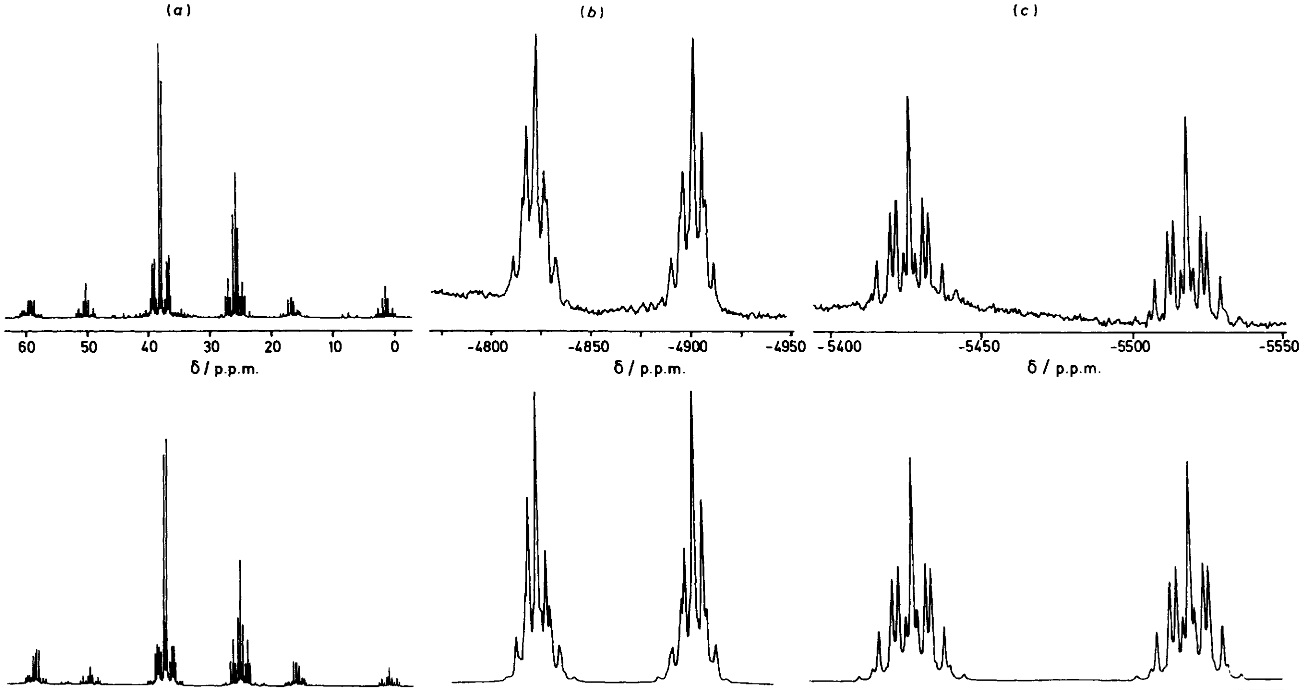

Figure 1. (*a*) Observed (upper) and calculated $^{31}P-\{^1H\}$ n.m.r. spectra for $[Pt_3(\mu-SO_2)_2(CNC_8H_9)_2\{P(C_6H_{11})_3\}_3]$. (*b*) Observed and calculated resonances for the Pt^2, $Pt^{2'}$ part of the corresponding $^{195}Pt-\{^1H\}$ spectrum. (*c*) Observed and calculated $^{195}Pt-\{^1H\}$ n.m.r. spectra for the remaining unique Pt atom Pt^1 (see Table 1 for atom labelling)

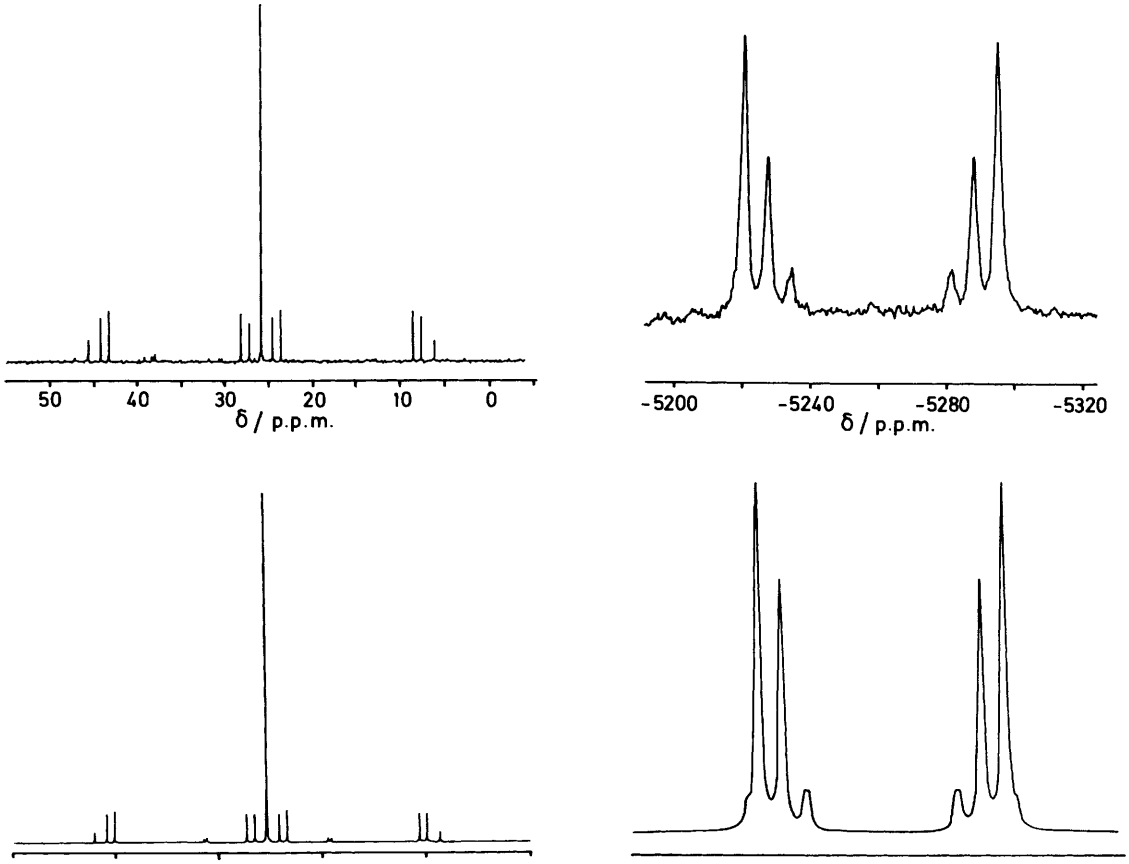

Figure 2. (*a*) Observed (upper) and calculated $^{31}P-\{^1H\}$ n.m.r. spectra for $[Pt_2(\mu-SO_2)(CNC_8H_9)_2\{P(C_6H_{11})_3\}_2]$. (*b*) Observed and calculated resonances for the corresponding $^{195}Pt-\{^1H\}$ n.m.r. spectrum

triangular cluster, $[Pt_3(\mu\text{-}SO_2)_2(CNC_8H_9)_2\{P(C_6H_{11})_3\}_3]$, and its yield reaches a maximum for the reaction of $[Pt_3(\mu\text{-}SO_2)_3\{P(C_6H_{11})_3\}_3]$ with 2 mol equivalents of 2,6-xylyl isocyanide. It reacts more slowly with a further mol of isocyanide to give the binuclear complex $[Pt_2(\mu\text{-}SO_2)(CNC_8H_9)_2\{P(C_6H_{11})_3\}_2]$ (**2**). Reaction of $[Pt_3(\mu\text{-}SO_2)_3\{P(C_6H_{11})_3\}_3]$ with 4—6 mol of isocyanide yields (**2**) plus unreacted ligand. Cluster degradation products are observed if the reactions are stirred for long periods of time.

Compound (**1**) is a red crystalline solid and its i.r. spectrum indicates the presence of terminal isocyanide (2 121 cm^{-1}) and bridging sulphur dioxide (1 132 and 1 020 cm^{-1}) ligands. The ^1H n.m.r. spectrum confirms the presence of 2,6-xylyl isocyanide and tricyclohexylphosphine ligands, in a ratio of 2:3, and suggests that the isocyanide ligands are equivalent in solution, because only one singlet is observed for the methyl groups. The $^{31}P\text{-}\{^1H\}$ n.m.r. spectrum, illustrated in Figure 1(*a*), is consistent with an asymmetric Pt_3P_3 triangle of C_{2v} symmetry. A satisfactory computer simulation of this spectrum has been achieved on the basis of such a system, comprising the isotopomers A_2B (29.6% abundance, no ^{195}Pt nuclei), AA′BX (29.6% abundance, one ^{195}Pt nucleus, X), A_2BY (14.8% abundance, one ^{195}Pt nucleus, Y), AA′BB′XX′ (14.8% abundance, two ^{195}Pt nuclei, X and X′), AA′BXY (7.4% abundance,

Table 1. Chemical shifts and coupling constants for $[Pt_3(\mu\text{-}SO_2)_2(CNC_8H_9)_2\{P(C_6H_{11})\}_3]$ (**1**)

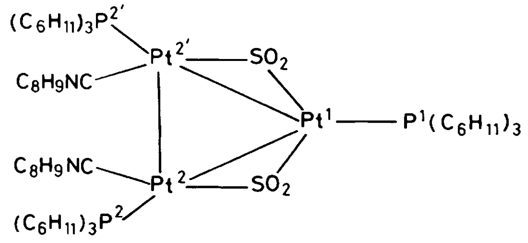

δ/p.p.m.			
P^1	P^2	Pt^1	Pt^2
26.0	38.1	−5 472	−4 861

	J/Hz				
	Pt^2	$Pt^{2'}$	Pt^1	P^2	$P^{2'}$
P^1	241	241	4 951	38	38
$P^{2'}$	242	4 296	242	55	
P^2	4 296	242	242		
Pt^1	697	697			
$Pt^{2'}$	920				

Table 2. Chemical shifts and coupling constants for $[Pt_2(\mu\text{-}SO_2)(CNC_8H_9)_2\{P(C_6H_{11})_3\}_2]$ (**2**)

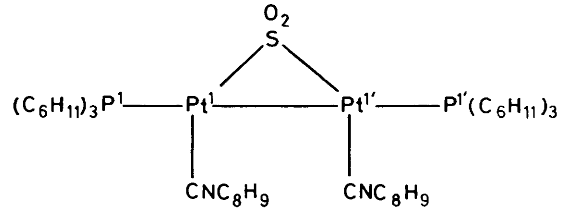

δ/p.p.m.	
P^1	Pt^1
26.0	−5 258

	J/Hz		
	Pt^1	Pt^1	P^1
P^1	3 624	375	91
P^1	375	3 624	
Pt^1	920		

Table 3. Structural details for $[Pt_3(\mu\text{-}SO_2)_2(CNC_8H_9)_2\{P(C_6H_{11})_3\}_3]\cdot 3MeCN\cdot CH_2Cl_2$ (**1**) and $[Pt_2(\mu\text{-}SO_2)(CNC_8H_9)_2\{P(C_6H_{11})_3\}_2]\cdot 1.5CH_2Cl_2$ (**2**)

	(**1**)	(**2**)
M	2 025.32	1 404.98
Space group	$P2_1$	$P2_1/n$
a/Å	14.957(5)	14.842(1)
b/Å	24.604(4)	25.394(3)
c/Å	13.035(2)	17.270(2)
β/°	114.28(2)	112.163(9)
U/Å^3	4 372.3	6 027.95
Z	2	4
F(000)	2 016	2 812
D_c/g cm^{-3}	1.52	1.55
μ/cm^{-1}	50.4	110.3
Radiation	Mo-K_α (λ = 0.710 69Å)	Cu-K_α (λ = 1.541 80 Å)
Scan technique	ω	ω
Scan width	0.9 + 0.35 tan θ	1.1 + tan θ
2θ range/°	3—50	3—130
Crystal decay	To 60%	To 90%
Absorption correction	Empirical	Empirical
maximum, minimum	1.18, 1.00	1.88, 1.00
No. reflections collected	7 805	10 602
No. reflections observed [$I > 3\sigma(I)$]	5 473	6 438
R_{merge}	0.0399	0.048
No. parameters varied	473	574
Weighting scheme	(1) 7.4	(1) 9.7
(Chebychev polynomial coefficients)	(2) −5.3	(2) −3.5
	(3) 4.5	(3) 6.9
R	0.0453	0.0461
R′	0.0488	0.0554

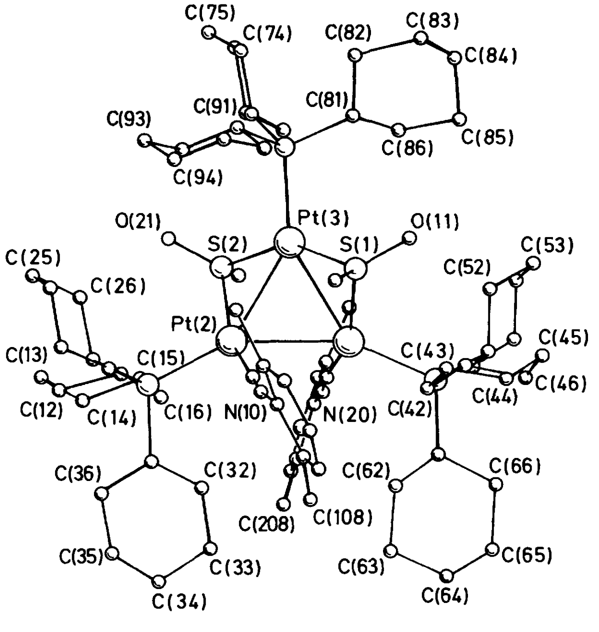

Figure 3. The molecular geometry of $[Pt_3(\mu\text{-}SO_2)_2(CNC_8H_9)_2\{P(C_6H_{11})_3\}_3]$

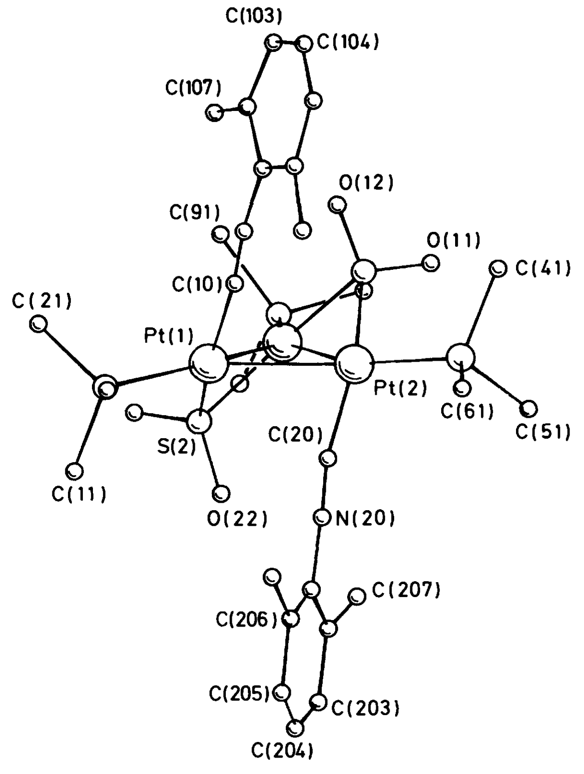

Figure 4. The inner co-ordination geometry of $[Pt_3(\mu\text{-}SO_2)_2(CNC_8H_9)_2\{P(C_6H_{11})_3\}_3]$

Table 4. Selected molecular dimensions (distances in Å, angles in °) for $[Pt_3(\mu\text{-}SO_2)_2(CNC_8H_9)_2\{P(C_6H_{11})_3\}_3]\cdot 3MeCN\cdot CH_2Cl_2$ with estimated standard deviations (e.s.d.s) in parentheses

Pt(1)–Pt(2)	2.8422(9)	Pt(1)–P(1)	2.294(4)
Pt(1)–Pt(3)	2.7282(9)	Pt(2)–P(2)	2.282(5)
Pt(2)–Pt(3)	2.7254(9)	Pt(3)–P(3)	2.263(6)
		Pt(1)–C(10)	1.98(2)
Pt(1)–S(2)	2.270(5)	Pt(2)–C(20)	1.96(2)
Pt(3)–S(2)	2.264(5)		
Pt(2)–S(1)	2.281(5)	C(10)–N(10)	1.13(2)
Pt(3)–S(1)	2.260(5)	C(20)–N(20)	1.15(2)
Pt(1)–Pt(3)–Pt(2)	62.82(3)	P(1)–Pt(1)–S(2)	100.2(2)
Pt(1)–Pt(2)–Pt(3)	58.64(3)	P(1)–Pt(1)–Pt(2)	152.4(1)
Pt(2)–Pt(1)–Pt(3)	58.54(2)	P(1)–Pt(1)–C(10)	98.9(5)
		C(10)–Pt(1)–S(2)	154.3(5)
P(3)–Pt(3)–S(1)	104.9(2)	C(10)–Pt(1)–Pt(2)	74.6(5)
P(3)–Pt(3)–S(2)	105.5(2)	S(2)–Pt(1)–Pt(2)	95.5(1)
S(1)–Pt(3)–S(2)	149.3(2)		
		P(2)–Pt(2)–S(1)	98.7(2)
Pt(1)–C(10)–N(10)	170.5(18)	P(2)–Pt(2)–Pt(1)	155.1(1)
Pt(2)–C(20)–N(20)	166.4(16)	P(2)–Pt(2)–C(20)	100.8(5)
		C(20)–Pt(2)–S(1)	154.9(5)
C(10)–N(10)–C(101)	171.9(19)	C(20)–Pt(2)–Pt(1)	74.0(5)
C(20)–N(20)–C(201)	172.8(22)	S(1)–Pt(2)–Pt(1)	94.3(1)

Table 5. Selected molecular dimensions (distances in Å, angles in °) for $[Pt_2(\mu\text{-}SO_2)(CNC_8H_9)_2\{P(C_6H_{11})_3\}_2]\cdot 1.5CH_2Cl_2$ with e.s.d.s in parentheses

Pt(1)–Pt(2)	2.6934(5)	Pt(1)–P(1)	2.309(2)
Pt(1)–S(1)	2.253(2)	Pt(2)–P(2)	2.317(2)
Pt(2)–S(1)	2.260(2)	Pt(1)–C(10)	1.96(1)
		Pt(2)–C(20)	1.96(1)
S(1)–O(1)	1.470(7)		
S(1)–O(2)	1.479(7)	C(10)–N(10)	1.18(1)
		C(20)–N(20)	1.16(1)
Pt(1)–S(1)–Pt(2)	73.29(7)	P(1)–Pt(1)–Pt(2)	155.47(6)
S(1)–Pt(1)–Pt(2)	53.48(6)	C(10)–Pt(1)–Pt(2)	100.7(3)
S(1)–Pt(2)–Pt(1)	53.23(6)	P(1)–Pt(1)–S(1)	102.03(8)
		C(10)–Pt(1)–S(1)	153.8(3)
Pt(1)–C(10)–N(10)	174.0(9)	P(1)–Pt(1)–C(10)	103.8(3)
Pt(2)–C(20)–N(20)	172.0(10)		
		P(2)–Pt(2)–Pt(1)	154.79(6)
C(10)–N(10)–C(11)	177.3(11)	C(20)–Pt(2)–Pt(1)	99.2(3)
C(20)–N(20)–C(21)	170.5(11)	P(2)–Pt(2)–S(1)	101.99(8)
		C(20)–Pt(2)–S(1)	151.2(3)
		P(2)–Pt(2)–C(20)	106.0(3)

two ^{195}Pt nuclei, X and Y), and AA′BXX′Y (3.7% abundance, three ^{195}Pt nuclei, X, X′, and Y).

The $^{195}Pt\text{-}\{^1H\}$ n.m.r. spectrum consists of two resonances, centred at −4 861 and −5 472 p.p.m. with respect to Na_2PtCl_6, which are illustrated in Figure 1(*b*) and (*c*). The former signal is essentially a doublet [^1J(Pt–P) = 4 296 Hz] with other fine structure, and arises from the two platinum atoms with co-ordinated isocyanide ligands. The latter signal is due to the remaining unique platinum atom and takes the form of a large doublet further split by overlapping triplets. Both resonances have been interpreted using the spin system described above and are consistent with the proposed structure of a C_{2v} Pt_3P_3 triangle. The coupling constants derived from the computer simulations of the $^{31}P\text{-}\{^1H\}$ and $^{195}Pt\text{-}\{^1H\}$ n.m.r. spectra of compound (**1**) are given in Table 1.

Compound (**2**) is a yellow, air-stable solid. The i.r. spectrum shows the presence of terminal isocyanide (2 115 and 2 088 cm^{-1}) and bridging sulphur dioxide (1 144 and 1 018 cm^{-1}) ligands. The ^1H n.m.r. spectrum exhibits resonances due to the 2,6-xylyl isocyanide and tricyclohexylphosphine ligands, in a 1:1 ratio, and only one singlet is observed for the methyl protons of the isocyanide.

The $^{31}P\text{-}\{^1H\}$ n.m.r. spectrum of (**2**) is illustrated in Figure 2(*a*). The spectrum has been satisfactorily simulated using a computer analysis based on a system comprising the isotopomers A_2 (44.4% abundance, no ^{195}Pt nuclei), AA′X

Table 6. Final fractional co-ordinates for compound (**1**) with e.s.d.s in parentheses

Atom	*X*/*a*	*Y*/*b*	*Z*/*c*
Pt(1)	1 034.0(5)	2 492(1)	4 242.3(5)
Pt(2)	2 285.3(5)	2 017(1)	3 337.6(6)
Pt(3)	1 972.1(5)	3 110(1)	3 250.9(6)
S(1)	3 441(3)	2 685(2)	3 994(4)
S(2)	346(3)	3 107(3)	2 836(4)
P(1)	−160(3)	2 444(3)	4 915(4)
P(2)	3 214(4)	1 346(2)	3 106(4)
P(3)	2 310(4)	3 962(3)	2 860(5)
O(11)	4 126(10)	2 734(6)	3 453(12)
O(12)	3 959(10)	2 724(6)	5 227(11)
O(21)	−88(12)	3 578(7)	3 136(14)
O(22)	−274(11)	2 908(7)	1 737(11)
N(10)	2 772(11)	2 053(8)	6 350(11)
N(20)	255(12)	1 567(8)	1 755(14)
C(10)	2 130(13)	2 169(8)	5 541(16)
C(20)	970(14)	1 725(7)	2 448(13)
C(11)	−1 366(15)	2 571(11)	3 796(16)
C(12)	−2 236(16)	2 664(10)	4 165(17)
C(13)	−3 196(20)	2 784(11)	3 170(23)
C(14)	−3 430(23)	2 378(12)	2 218(26)
C(15)	−2 623(23)	2 343(12)	1 802(25)
C(16)	−1 625(19)	2 169(11)	2 843(22)
C(21)	−8(14)	2 932(8)	6 033(16)
C(22)	967(18)	2 851(10)	7 045(21)
C(23)	1 073(24)	3 268(15)	7 998(28)
C(24)	1 031(26)	3 818(15)	7 594(30)
C(25)	91(28)	3 931(16)	6 641(32)
C(26)	−59(21)	3 514(13)	5 643(26)
C(31)	−223(17)	1 775(9)	5 510(20)
C(32)	101(25)	1 336(14)	5 094(28)
C(33)	203(22)	781(12)	5 635(25)
C(34)	−329(26)	714(15)	6 394(30)
C(35)	−586(26)	1 161(14)	6 771(29)
C(36)	−722(20)	1 704(11)	6 251(22)
C(41)	4 552(14)	1 432(8)	4 046(16)
C(42)	4 723(19)	1 425(11)	5 306(21)
C(43)	5 772(18)	1 582(10)	6 068(20)
C(44)	6 485(21)	1 266(12)	5 831(24)
C(45)	6 331(20)	1 277(11)	4 623(23)
C(46)	5 311(19)	1 095(11)	3 870(23)
C(51)	3 249(15)	1 338(9)	1 718(17)
C(52)	3 529(18)	1 882(10)	1 450(21)
C(53)	3 498(25)	1 885(14)	227(30)
C(54)	2 433(24)	1 739(14)	−621(28)
C(55)	2 160(26)	1 241(15)	−365(31)
C(56)	2 169(20)	1 208(11)	804(23)
C(61)	2 859(22)	678(12)	3 302(25)
C(62)	2 179(29)	573(16)	3 644(33)
C(63)	1 929(20)	26(11)	4 056(23)
C(64)	2 340(29)	−419(17)	3 641(33)
C(65)	2 962(35)	−362(19)	3 211(38)
C(66)	3 318(17)	194(10)	2 961(20)
C(71)	1 224(16)	4 317(10)	1 829(19)
C(72)	765(18)	3 997(10)	710(21)
C(73)	−273(19)	4 246(11)	−14(22)
C(74)	−152(23)	4 852(13)	−223(26)
C(75)	358(20)	5 150(11)	851(22)
C(76)	1 342(19)	4 911(11)	1 623(21)
C(81)	3 340(19)	3 972(11)	2 430(23)
C(82)	3 760(32)	4 510(18)	2 369(36)
C(83)	4 774(35)	4 410(20)	2 131(42)
C(84)	4 505(49)	4 066(28)	1 244(59)
C(85)	4 106(30)	3 497(18)	1 204(34)
C(86)	3 128(22)	3 618(13)	1 341(25)
C(91)	2 711(18)	4 390(10)	4 217(20)
C(92)	1 878(17)	4 405(10)	4 526(20)
C(93)	2 190(26)	4 689(15)	5 660(30)
C(94)	3 211(24)	4 458(13)	6 525(27)
C(95)	3 932(21)	4 444(12)	6 208(24)
C(96)	3 675(19)	4 154(11)	5 074(22)
C(101)	3 642(15)	1 933(8)	7 266(18)
C(102)	4 217(15)	2 366(8)	7 920(17)
C(103)	5 133(18)	2 209(10)	8 817(21)
C(104)	5 343(20)	1 680(12)	9 034(21)
C(105)	4 782(21)	1 273(12)	8 484(23)
C(106)	3 902(17)	1 385(10)	7 553(19)
C(107)	3 896(18)	2 950(10)	7 564(21)
C(108)	3 224(18)	944(10)	6 932(21)
C(201)	−651(16)	1 444(9)	880(18)
C(202)	−912(18)	1 715(10)	−134(21)
C(203)	−1 830(21)	1 547(12)	−1 012(24)
C(204)	−2 366(22)	1 175(12)	−828(25)
C(205)	−2 106(22)	877(13)	139(26)
C(206)	−1 182(19)	1 015(11)	1 069(22)
C(207)	−263(20)	2 118(13)	−319(23)
C(208)	−913(22)	721(13)	2 161(26)
Cl(1)	7 947(19)	4 796(12)	1 485(22)
Cl(2)	7 665(19)	4 353(12)	3 226(23)
N(1)	−2 168(25)	3 095(15)	−538(28)
N(2)	7 812(22)	2 877(13)	7 021(25)
N(3)	4 576(30)	51(17)	626(30)
C(1)	8 033(41)	4 206(24)	2 248(51)
C(2)	−2 770(35)	3 402(18)	−615(38)
C(3)	−3 641(39)	3 745(22)	−841(51)
C(4)	7 056(23)	3 017(13)	6 434(22)
C(5)	6 049(23)	3 185(17)	5 684(28)
C(6)	5 316(34)	283(18)	948(27)
C(7)	6 095(39)	696(22)	1 460(45)

(44.4% abundance, one ^{195}Pt nucleus, X), and AA′XX′ (11.1% abundance, two ^{195}Pt nuclei, X and X′). The ^{195}Pt-{^{1}H} n.m.r. spectrum is illustrated in Figure 2(*b*) and has also been interpreted using the spin system described above. Low-intensity signals due to the AA′XX′ isotopomer were observed and allowed ^{1}J(Pt–Pt) to be calculated. The coupling constants derived from the computer simulations of the ^{31}P-{^{1}H} and ^{195}Pt-{^{1}H} n.m.r. spectra are given in Table 2. Both spectra are consistent with a Pt_2P_2 system where the phosphorus atoms occupy symmetrically equivalent sites and the large value of ^{3}J(P–P) suggests a *trans*-PPtPtP geometry.

In order to confirm the structures of both compounds, single-crystal *X*-ray crystallographic analyses were completed on (**1**) and (**2**). Details are summarised in Table 3 and in the Experimental section. Selected intramolecular bond lengths and angles for both molecules are given in Tables 4 and 5, and fractional co-ordinates of the non-hydrogen atoms in Tables 6 and 7.

The molecular structure of (**1**) is illustrated in Figures 3 and 4, and consists of an isosceles triangle of platinum atoms, with Pt–Pt distances of 2.7254(9), 2.7282(9), and 2.8422(9) Å, and angles of 58.54(2), 58.64(3), and 62.82(3)°. The shorter Pt–Pt edges are bridged by sulphur dioxide ligands, while the longer Pt–Pt edge is unbridged. The Pt–Pt distances lie towards the upper range of distances found for *triangulo*-platinum cluster compounds.[6] This can be attributed to the large size of the bridging sulphur atoms, since Pt–Pt distances in such clusters are found to depend approximately on the size of the bridging ligands. Compound (**1**) is a 44-electron *triangulo*-platinum cluster, and the Pt–Pt bond lengths in such compounds are generally longer than those for comparable 42-electron clusters. Thus the Pt–Pt distances in (**1**) are similar to those reported for the isoelectronic compound $[Pt_3(\mu\text{-}SO_2)_3\{P(C_6H_{11})_3\}_2(dppp)]$[dppp = 1,3-bis(diphenylphosphino)propane].[5]

The phosphorus atoms are all approximately coplanar with

Table 7. Final fractional co-ordinates for compound (**2**) with e.s.d.s in parentheses

Atom	*X*/*a*	*Y*/*b*	*Z*/*c*	Atom	*X*/*a*	*Y*/*b*	*Z*/*c*
Pt(1)	2 685.4(3)	608.9(1)	1 272.2(2)	C(43)	5 526(11)	−188(6)	3 879(9)
Pt(2)	2 680.6(3)	1 108.1(2)	−105.3(2)	C(44)	6 189(10)	259(7)	3 817(8)
S	2 858(2)	1 480.9(9)	1 132(1)	C(45)	5 810(10)	782(7)	3 948(9)
P(1)	2 828(2)	546.0(9)	2 647(1)	C(46)	4 758(9)	870(5)	3 312(8)
P(2)	2 624(2)	1 838.7(9)	−927(2)	C(51)	2 159(8)	−22(4)	2 827(6)
O(1)	2 066(6)	1 811(3)	1 177(5)	C(52)	1 088(8)	−43(4)	2 240(7)
O(2)	3 832(6)	1 709(3)	1 586(5)	C(53)	644(9)	−567(5)	2 317(8)
N(10)	2 105(7)	−534(3)	578(5)	C(54)	713(13)	−654(6)	3 188(10)
N(20)	2 852(6)	132(4)	−1 131(5)	C(55)	1 761(12)	−634(5)	3 800(8)
C(10)	2 378(7)	−110(4)	847(6)	C(56)	2 225(10)	−107(5)	3 728(7)
C(20)	2 715(8)	494(5)	−782(7)	C(61)	1 431(8)	2 169(4)	−1 341(7)
C(11)	1 806(8)	−1 027(3)	235(6)	C(62)	644(9)	1 804(5)	−1 918(8)
C(12)	2 518(7)	−1 376(4)	190(7)	C(63)	−356(9)	2 074(6)	−2 296(8)
C(13)	2 170(10)	−1 864(5)	−167(8)	C(64)	−647(9)	2 280(6)	−1 624(9)
C(14)	1 208(10)	−1 992(5)	−470(8)	C(65)	105(11)	2 633(7)	−1 052(10)
C(15)	527(8)	−1 643(4)	−429(7)	C(66)	1 087(10)	2 358(6)	−665(8)
C(16)	817(7)	−1 145(4)	−64(6)	C(71)	2 890(8)	1 685(4)	−1 867(6)
C(17)	3 565(9)	−1 219(5)	500(9)	C(72)	3 861(10)	1 448(5)	−1 693(8)
C(18)	75(9)	−765(5)	−15(9)	C(73)	3 981(12)	1 247(6)	−2 481(9)
C(21)	3 067(8)	−338(4)	−1 417(6)	C(74)	3 775(13)	1 669(7)	−3 126(9)
C(22)	2 330(10)	−713(5)	−1 732(8)	C(75)	2 849(13)	1 928(7)	−3 304(9)
C(23)	2 612(16)	−1 200(5)	−1 966(11)	C(76)	2 733(11)	2 136(6)	−2 509(9)
C(24)	3 546(17)	−1 304(7)	−1 893(12)	C(81)	3 449(9)	2 365(4)	−305(7)
C(25)	4 241(13)	−930(7)	−1 585(10)	C(82)	3 353(12)	2 921(5)	−681(11)
C(26)	4 046(10)	−428(5)	−1 354(7)	C(83)	3 972(15)	3 305(6)	10(12)
C(27)	1 321(11)	−588(6)	−1 828(9)	C(84)	5 001(14)	3 141(7)	387(11)
C(28)	4 802(10)	3(7)	−1 085(9)	C(85)	5 133(10)	2 596(7)	715(9)
C(31)	2 459(7)	1 163(4)	3 032(6)	C(86)	4 522(9)	2 193(5)	59(8)
C(32)	2 805(11)	1 241(5)	3 997(7)	Cl(1)	1 894(5)	3 304(3)	2 594(4)
C(33)	2 549(12)	1 786(5)	4 182(8)	Cl(2)	791(6)	3 398(3)	873(5)
C(34)	1 483(12)	1 912(5)	3 748(9)	Cl(3)	5 306(22)	4 713(13)	−37(20)
C(35)	1 139(10)	1 831(5)	2 799(9)	Cl(4)	6 707(27)	4 670(17)	1 430(21)
C(36)	1 377(8)	1 267(4)	2 602(8)	C(1)	1 677(15)	3 042(8)	1 604(13)
C(41)	4 085(8)	427(4)	3 377(6)	C(2)	5 964(29)	5 090(12)	781(24)
C(42)	4 502(9)	−97(5)	3 247(8)				

the platinum triangle, but the sulphur dioxide and isocyanide ligands lie out of this plane and in a transoid arrangement with respect to one another. A similar geometry has been observed in $[Pt_3(\mu\text{-}SO_2)_3\{P(C_6H_{11})_3\}_2(dppp)]$.[5] The isocyanide ligands are effectively linear (av. C–N–C 172°). The platinum–phosphorus bond lengths are seen to vary within the molecule, the Pt–P distance to the unique platinum atom being shorter than that to the two symmetry-equivalent platinum atoms. There is also a slight asymmetry in the Pt–S distances. Both effects may be due, in part, to the π-acid properties of the isocyanide ligands co-ordinated to the two equivalent platinum atoms.

The structure of (**1**) has no precedent in platinum cluster chemistry and represents the first example of a *triangulo*-platinum cluster compound with less than three edge-bridging ligands. Such a structure has, however, been observed previously in the related palladium isocyanide *triangulo*-cluster compounds $[Pd_3(\mu\text{-}SO_2)_2(CNBu^t)_5]$[7] and $[Pd_3(\mu\text{-}SO_2)_2(CNC_8H_9)_2\{P(C_6H_{11})_3\}_3]$.[8] As we have discussed previously,[5] if the bridged metal–metal bonds are ignored, then these

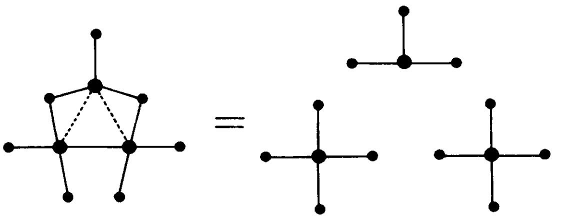

Scheme 2.

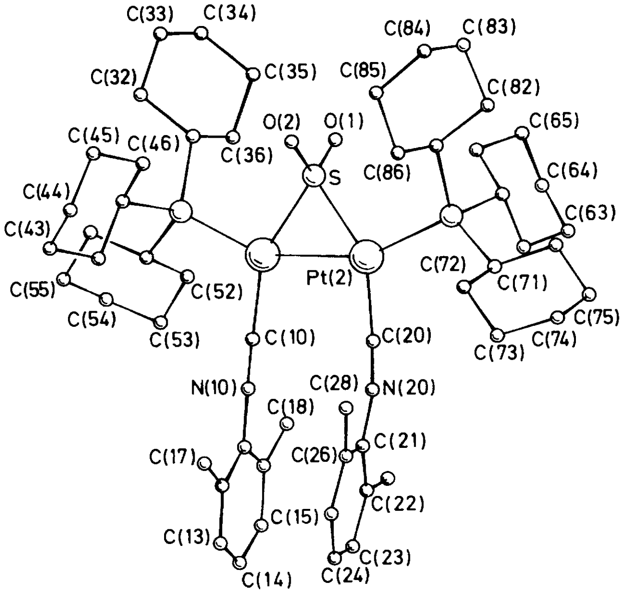

Figure 5. The molecular geometry of $[Pt_2(\mu\text{-}SO_2)(CNC_8H_9)_2\{P(C_6H_{11})_3\}_2]$

molecules can be built up from two square-planar ML_4 fragments and one T-shaped ML_3 fragment (see Scheme 2). Severe steric overcrowding and the bond-angle requirements at the platinum atoms prevent such a system from adopting a planar $M_3(\mu\text{-}X)_2$ ring, and the observed folded geometry is preferred. The related isocyanide cluster compound $[Pt_3(CNC_8H_9)_6(PPh_3)_2]^{2+}$ also has 44 valence electrons, but a linear Pt–Pt–Pt skeleton.[9] At each metal atom the geometry is square planar and all the ligands are terminal.

The crystal structure of compound (**2**), which is illustrated in Figure 5, confirms the spectroscopic data collected for it. The compound is a binuclear platinum species containing a *trans* arrangement of phosphine ligands, with a bridging sulphur dioxide group and terminal isocyanide ligands completing the co-ordination geometry about each platinum. All of the metal-bound atoms are approximately coplanar with the Pt_2S triangle, although the isocyanide ligands lie slightly out of the plane, with one above and one below (the C–N vector makes an angle of 8° with this plane) and with their phenyl rings tilted at an angle of 67° to the Pt_2S triangle. A C_2 axis bisects the Pt–Pt bond and the sulphur atom, rendering both phosphine and both isocyanide ligands symmetry equivalent. The isocyanide ligands are effectively linear [C–N–C 177.3(11) and 170.5(11)°] and there are no anomalous metal–ligand distances.

The Pt–Pt distance is 2.6934(5) Å. This can be compared to those in the isoelectronic sulphur-bridged platinum dimers $[Pt_2(\mu\text{-}S)(PPh_3)_3(CO)]$[10] and $[Pt_2(\mu\text{-}S)(2,4,6\text{-}Bu^t{}_3C_6H_2NC)_4]$,[11] 2.647(2) and 2.604(2) Å respectively. In both of these compounds the Pt–Pt distances are considered representative of a single covalent Pt–Pt bond. The formalism of a single Pt–Pt bond in (**2**) satisfies the requirement of a sixteen-electron environment about each platinum atom.

The very different substitutional behaviour of $[Pt_3(\mu\text{-}CO)_3\{P(C_6H_{11})_3\}_3]$ and $[Pt_3(\mu\text{-}SO_2)_3\{P(C_6H_{11})_3\}_3]$ towards CNC_8H_9 is very striking. In the former case the introduction of a bridging CNC_8H_9 ligand labilises an adjacent phosphine, whereas in the latter the CNC_8H_9 ligand retains a terminal position and no phosphine labilisation occurs. Therefore, the SO_2 clusters appear to be more susceptible to cluster degradation than the CO clusters. The electronic and steric factors responsible for these differences are difficult to evaluate and clearly more kinetic and spectroscopic data are required to resolve the problem.

Experimental

All reactions were performed using standard Schlenk-line procedures under an atmosphere of pure, dry nitrogen and using dry, oxygen-free solvents. Microanalyses were carried out by Mr. M. Gascoyne and his staff of this laboratory. Infra-red spectra were recorded as Nujol mulls and in CH_2Cl_2 solution using a Perkin-Elmer 1700FT spectrometer.

Proton n.m.r. spectra were obtained on a Brüker WH300 spectrometer. Proton-decoupled ^{31}P and ^{195}Pt n.m.r. spectra were recorded using a Brüker AM-250 spectrometer, operating at frequencies of 101.26 and 53.55 MHz respectively. Samples for $^{31}P\text{-}\{^1H\}$ were referenced to $PO(OMe)_3$ in D_2O and $^{195}Pt\text{-}\{^1H\}$ samples to Na_2PtCl_6 in D_2O. All n.m.r. samples were run in CD_2Cl_2. N.m.r. computer simulations were carried out using the Oxford University VAX computer system, utilising a program developed by Dr. R. K. Harris of the University of East Anglia and adapted for use at Oxford by Dr. A. E. Derome.

The complex $[Pt_3(\mu\text{-}SO_2)_3\{P(C_6H_{11})_3\}_3]$ was synthesised by standard literature methods.[4]

Synthesis of $[Pt_3(\mu\text{-}SO_2)_2(CNC_8H_9)_2\{P(C_6H_{11})_3\}_3]$ (**1**).—A solution of 2,6-xylyl isocyanide (0.0650 g, 0.495 mmol) in benzene (20 cm^3) was added with stirring to a solution of $[Pt_3(\mu\text{-}SO_2)_3\{P(C_6H_{11})_3\}_3]$ (0.40 g, 0.247 mmol) in benzene (20 cm^3). The deep red solution immediately lightened in colour and stirring was continued for a further 20 min. Orange microcrystals of compound (**1**) were obtained by recrystallisation from CH_2Cl_2–CH_3CN (0.31 g, 69%) (Found: C, 46.0; H, 6.4; N, 1.6. $C_{72}H_{117}N_2O_4P_3Pt_3S_2\cdot CH_2Cl_2$ requires C, 46.1; H, 6.3; N, 1.5%). I.r. (Nujol): ν(CN) at 2 121s cm^{-1} and ν(SO_2) at 1 132m and 1 020s cm^{-1}. Proton n.m.r. (CD_2Cl_2): δ 7.18—7.05 (m, 6 H, C_6H_3NC), 2.47 (s, 12 H, CH_3), and 2.11—1.23 (m, 99 H, C_6H_{11}). Details of the $^{31}P\text{-}\{^1H\}$ and $^{195}Pt\text{-}\{^1H\}$ n.m.r. studies are summarised in Table 1.

Synthesis of $[Pt_2(\mu\text{-}SO_2)(CNC_8H_9)_2\{P(C_6H_{11})_3\}_2]$ (**2**).—A solution of 2,6-xylyl isocyanide (0.0486 g, 0.371 mmol) in benzene (20 cm^3) was added with stirring to a solution of $[Pt_3(\mu\text{-}SO_2)_3\{P(C_6H_{11})_3\}_3]$ (0.20 g, 0.124 mmol) in benzene (10 cm^3). The deep red solution immediately lightened in colour, and stirring was continued for 1 h to yield an orange solution. The solvent was removed *in vacuo*, and compound (**2**) obtained as a yellow powder by taking up the reaction mixture in diethyl ether and reducing the volume to *ca.* 5 cm^3. More (**2**) (total 0.16 g, 68%) was obtained by repeatedly taking up the filtrate in diminishing amounts of diethyl ether (Found: C, 50.7; H, 6.8; N, 2.0. $C_{54}H_{84}N_2O_2P_2Pt_2S$ requires C, 50.8; H, 6.6; N, 2.2%). I.r. (Nujol):ν(CN) at 2 115s and 2 088m (sh) cm^{-1} and ν(SO_2) at 1 144m and 1 018m cm^{-1}; (CH_2Cl_2):ν(CN) at 2 115s cm^{-1} and ν(SO_2) at 1 015 cm^{-1}. Proton n.m.r. (CD_2Cl_2): δ 6.88—6.83 (m, 2 H, *p*-C_6H_3NC), 6.74—6.72 (m, 4 H, *m*-C_6H_3NC), 2.18 (s, 12 H, CH_3), and 2.08—1.21 (m, 66 H, C_6H_{11}). Details of the $^{31}P\text{-}\{^1H\}$ and $^{195}Pt\text{-}\{^1H\}$ n.m.r. studies are summarised in Table 2.

Crystal Structure Determination of Compound (**1**).—Crystals of compound (**1**) were grown as orange parallelepipeds by layer diffusion of acetonitrile into a dichloromethane solution of the compound at room temperature. A crystal of approximate dimensions 0.25 × 0.1 × 0.1 mm was taken directly from this solution and sealed in a 0.3-mm Lindemann capillary tube with a small quantity of the mother-liquor. Diffraction data were collected on an Enraf-Nonius CAD4 diffractometer at room temperature (23 °C). Details of the data collection and refinement are summarised in Table 3.

The crystal quality was deemed to be acceptable after checking several strong low-angle reflections by taking open canter ω scans ($\Delta\omega_{\frac{1}{2}} = 0.3°$). The Laue symmetry ($2/m$) and the systematic absences ($0k0$, $k = 2n + 1$) were consistent with either of the monoclinic space groups $P2_1$ (no. 4) or $P2_1/m$ (no. 11).

The positions of the platinum atoms obtained from the Patterson map did not help to distinguish between these two possibilities, a platinum triangle was revealed which had either true crystallographic or pseudo-mirror symmetry. Refinement and Fourier difference syntheses in the centrosymmetric space group did not lead to a sensible solution. Initial refinement in $P2_1$ was hampered by the pseudo-mirror symmetry of the heavy atoms. The ill conditioning of the least-squares matrix was broken by defining four new parameters based on the sum and difference of the x and z co-ordinates of the two platinums related by the pseudo-mirror. Three cycles of refinement with fixed thermal parameters led to a decrease in the R value from 0.23 to 0.16. The platinum atoms were sufficiently displaced from their original positions that the resulting Fourier difference map did not possess mirror symmetry, although 'ghost' peaks could be discerned for certain atoms. Input of the top five peaks as three phosphorus and two sulphur atoms led to a much better phasing model, because one sulphur did not lie close to the pseudo-mirror or have a counterpart related by the pseudo-symmetry. All non-hydrogen atoms of the molecule were subsequently located from Fourier difference maps. After isotropic refinement an R value of 0.0801 was attained. A number of residual peaks appeared in the Fourier map which were not associated with the main molecule. The top two were approximately 3.5 e Å^{-3} in height and were modelled as the chlorines of a dichloromethane molecule. Ten other peaks which were between 1.0 and 2.0 e Å^{-3} appeared to be chemically sensible, one as the carbon of the dichloromethane and the others as three linear residues, modelled as acetonitrile molecules.

Platinum atoms and atoms of the co-ordination sphere were refined with anisotropic thermal parameters and the remaining non-hydrogen atoms isotropically. Hydrogen atoms were placed in calculated positions ($d_{\text{C-H}}$ = 1.00 Å, U_{iso} = 0.1 Å^2).

Crystal Structure Determination of Compound (**2**).—Crystals of compound (**2**) were grown as yellow parallelepipeds by evaporation of a saturated CH_2Cl_2–hexane solution of the compound over a period of weeks. A bar-shaped specimen of dimensions 0.45 × 0.15 × 0.075 mm was mounted in a similar way to that of compound (**1**). Crystal quality was comparable to that of (**1**). The Laue symmetry was found to be $2/m$ and the systematic absences $0k0$, $k = 2n + 1$, $h0l$ and $h + l = 2n + 1$ uniquely determined the space group as $P2_1/n$.

Data were collected, as for (**1**), by the ω-scan technique, using Cu-K_α radiation. Details of the data collection and refinement are summarised in Table 4. The structure solution was more straightforward than for (**1**). Excepting those of solvent molecules, all non-hydrogen atoms were rapidly located after solution of the Patterson function yielded the position of the Pt atoms. Two large peaks of residual electron density (*ca.* 5.5 e Å^{-3}) remained with a third (2.5 e Å^{-3}) which was approximately 3.0 Å from one of the SO_2 oxygen atoms. These three were obviously atoms of a dichloromethane molecule which was weakly hydrogen-bonded to the sulphur dioxide. Three other peaks between 1.0 and 2.0 e Å^{-3} were then located near the inversion centre ($\frac{1}{2}$, $\frac{1}{2}$, 0). These could only be modelled as a further dichloromethane residue in 50% occupancy, which was refined with restraints.

All non-hydrogen atoms were refined anisotropically with the exception of the solvent atoms. The maximum residual electron density was 1.2 e Å^{-3} located close to Cl(1).

The calculations for the two crystallographic determinations described above were completed using the CRYSTALS suite of computer programs.[12]

Additional material available from the Cambridge Crystallographic Data Centre comprises thermal parameters and remaining bond lengths and angles.

References

1 C. E. Briant, D. I. Gilmour, D. M. P. Mingos, and R. W. M. Wardle, *J. Chem. Soc., Dalton Trans.*, 1985, 1693.

2 A. Albinati, *Inorg. Chim. Acta*, 1977, **22**, L31; D. C. Moody and R. R. Ryan, *Inorg. Chem.*, 1977, **16**, 1052; M. Green, J. A. K. Howard, M. Murray, J. L. Spencer, and F. G. A. Stone, *J. Chem. Soc., Dalton Trans.*, 1977, 1509; P. W. Frost, J. A. K. Howard, J. L. Spencer, D. G. Turner, and D. Gregson, *J. Chem. Soc., Chem. Commun.*, 1981, 1104; A. Albinati, G. Carturan, and A. Musco, *Inorg. Chim. Acta*, 1976, **16**, L3; G. Longoni and P. Chini, *J. Am. Chem. Soc.*, 1976, **98**, 7225; N. J. Taylor, P. C. Chieh, and A. J. Carty, *J. Chem. Soc., Chem. Commun.*, 1975, 448.

3 C. S. Browning, D. H. Farrar, R. R. Gukathasan, and S. A. Morris, *Organometallics*, 1985, **4**, 1750.

4 C. E. Briant, D. G. Evans, and D. M. P. Mingos, *J. Chem. Soc., Chem. Commun.*, 1982, 1144.

5 M. F. Hallam, N. D. Howells, D. M. P. Mingos, and R. W. M. Wardle, *J. Chem. Soc., Dalton Trans.*, 1985, 845.

6 D. M. P. Mingos and R. W. M. Wardle, *Transition Met. Chem. (Weinheim, Ger.)*, 1985, **10**, 441.

7 S. Otsuka, Y. Tatsuno, M. Niki, T. Aoki, M. Matsumoto, H. Yoskioka, and K. Nakatsu, *J. Chem. Soc., Chem. Commun.*, 1973, 445.

8 S. G. Bott, O. Ezomo, D. M. P. Mingos, and I. D. Williams, unpublished work.

9 C. E. Briant, D. I. Gilmour, and D. M. P. Mingos, *J. Organomet. Chem.*, 1986, **308**, 381.

10 A. C. Skapski and P. G. H. Troughton, *J. Chem. Soc. A*, 1969, 2772.

11 Y. Yamamoto and H. Yamazaki, *J. Chem. Soc., Dalton Trans.*, 1986, 677.

12 D. J. Watkin, J. R. Caruthers, and B. W. Bethridge, CRYSTALS user guide, Chemical Crystallographic Laboratory, Oxford, 1985.

Received 12th August 1987; *Paper* 7/1484